Calculation of Anharmonic IR and Raman Intensities for Periodic Systems from DFT Calculations: Implementation and Validation

Calculation of Anharmonic IR and Raman Intensities for Periodic Systems from DFT Calculations: Implementation and Validation

P. Carbonnière,[1,*] A. Erba,[2] F. Richter[1], R. Dovesi,[2] and M. Rerat[1]

[1]IPREM, Université de Pau et des Pays de l'Adour, IPREM-CAPT UMR CNRS 5254, Hélioparc Pau Pyrénées, 2 avenue du Président Angot, 64053 Pau Cedex 09, Pau, France

[2]Dipartimento di Chimica, Università di Torino, via Giuria 5, 10125, Torino, Italy

KEYWORDS: IR and Raman spectra, periodic systems, Anharmonic intensities, Variational wavefunction, DFT.

ABSTRACT: An extension of the CRYSTAL program is presented allowing for calculations of anharmonic Infrared (IR) intensities and Raman activities for periodic systems. This work is a follow up of two papers devoted to the computation of anharmonic vibrational states of solids from DFT calculations, part I: description of the potential energy surface (J. Chem. Theory Comput. 15 (2019) 3755-3765) and part II: implementation of the VSCF and VCI methods (J. Chem. Theory Comput. 15 (2019) 3766-3777). The approach presented here relies on the evaluation of integrals of the dipole moment and polarizability operators over anharmonic wavefunctions obtained from either VSCF or VCI calculations. With this extension, the program now allows for a more complete characterization of the vibrational spectroscopic features

of solids within the density functional theory. In particular, it is able (i) to provide reliable positions and intensities for most intense spectral features, and (ii) to check whether a first overtone or a combination band has a non-vanishing IR intensity or Raman activity. Therefore, it becomes possible to assign the transition(s) corresponding to satellite peak(s) around a fundamental transition, or the overtones or combination bands that may be as intense as their corresponding fundamental transitions through the strongest mode-mode couplings, as in so-called Fermi resonances. The present method is assessed on two molecular systems, H_2O and H_2CO, as well as on two solid state cases, Boron hydrides BH_4 and their deuterated species BD_4 in a crystalline environment of alkali metals (M=Na, K). The solid state cases are particularly insightful as, in the B-H (or B-D) stretching region here considered, they exhibit many spectral features entirely due to anharmonic effects: two out of three in the IR spectrum and four out of six in the Raman spectrum. All IR and Raman active overtones and combination bands experimentally observed are correctly predicted with our approach. The effect of the adopted quantum-chemical model (DFT exchange-correlation functional/basis set) for the electronic structure calculations on the computed spectra is discussed and found to be significant, which suggests some special care is needed for the analysis of subtle spectral features.

INTRODUCTION

The complete IR and Raman characterization of a compound may require not only the correct identification of the fundamental transitions but also the identification of their active overtones or combination bands. This allows to identify all of the vibrational signatures of the compound of interest or to extract the signature of a particular molecular fragment within a more chemically complex material/environment[i].

These intrinsically anharmonic spectral features (overtones and combination bands) may complicate the assignment. Despite being mainly observed in the X-H stretching region (X being any atom but H),[ii,iii] they can be found at any spectral range. For instance, they appear around 850 cm^{-1} for carbonate minerals for which the assignment is still open to debate[iv,v].

From a theoretical point of view, their description requires to go beyond the usual harmonic approximation by considering the so-called mechanical anharmonicity and, to a lesser extent, the electrical anharmonicity. Both of them may provide a non-null contribution to IR intensities and Raman activities of the overtones and combination bands. The former takes mode-mode couplings into account, which arise from anharmonic terms of the potential energy surface (PES), while the latter is related to the anharmonic terms of the dipole moment (IR) or induced dipole moment (Raman). Formally, in terms of Taylor's expansions up to the n^{th} order (in the basis of normal mode coordinates) of the PES and dipole moment (here both truncated to two-mode terms for brevity), the mechanical anharmonicity is related to the terms beyond the second order in **equation (1)** while the electrical anharmonicity corresponds to the terms beyond the first order in **equation (2):**

$$V_{(Q_1,Q_2,\ldots,Q_m)} = \sum_{p}^{n} \sum_{i}^{\square} \frac{1}{p!} \frac{\partial^p V}{\partial Q_i^p} Q_i^p + \sum_{p,q}^{p+q=n} \sum_{i,j\neq i}^{\square} \frac{1}{p!\,q!} \frac{\partial^{(p+q)} V}{\partial Q_i^p \partial Q_j^q} Q_i^p Q_j^q + \cdots \quad (1)$$

$$\mu_{a(Q_1,Q_2,\ldots,Q_m)} = \mu_{0_a} + \sum_{p}^{n} \sum_{i}^{\square} \frac{1}{p!} \frac{\partial^p \mu_a}{\partial Q_i^p} Q_i^p + \sum_{p,q}^{p+q=n} \sum_{i,j\neq i}^{\square} \frac{1}{p!\,q!} \frac{\partial^{(p+q)} \mu_a}{\partial Q_i^p \partial Q_j^q} Q_i^p Q_j^q + \cdots \quad (2)$$

Above, Q_i is the i^{th} normal mode coordinate of the system, μ_a is the dipole moment along the Cartesian axis a, and V the potential energy of the system.

Although the related methodological aspects are already discussed in the literature for polyatomic molecules, they were yet to be implemented in softwares for the modeling of periodic systems. The present paper indeed focuses on the anharmonic computation of IR intensities and Raman activities for periodic systems. More precisely, it involves the implementation of the evaluation of integrals of the dipole moment and polarizability operators over the anharmonic vibrational wavefunctions obtained from VSCF (Vibrational Self-Consistent Field) or VCI (Vibrational Configuration Interaction) calculations. With this extension, the program now allows for a more complete characterization of the vibrational spectroscopic features of solids within the density functional theory. In particular, it is able (i) to provide reliable positions and intensities for most intense spectral features, and (ii) to check whether a first overtone or a combination band has a non-vanishing IR intensity or Raman activity.

Theoretical results on the two chosen molecular systems, water H_2O and formaldehyde H_2CO, will be reported first and compared to the literature[vi,vii]. Simulated IR and Raman spectra will then be illustrated on periodic systems with the case of $BH(D)_4$- species in a crystalline environment of Na and K alkali metal ions. Due to strong anharmonic couplings in the B-H stretching region, the number of active bands is three times the number of active fundamental transitions provided by the harmonic approximation[viii]. Face centered cubic $MBH(D)_4$ (M=Na,K) is also a small sized system of six atoms per cell for which the computation of the PES along the librational modes (inter-mode couplings between $BH(D)_4$ species and the alkali metal M) can be avoided because there are no strong interactions with the internal modes of $BH(D)_4$[ix]. This yields a nine-dimensional PES surface, which does not exhibit low frequency modes (below

400 cm^{-1}). Therefore, truncation of the PES expansion to fourth-order ensures a correct mathematical representation of the vibrational motions related to the $BH(D)_4$ part of the system.

METHODOLOGICAL ASPECTS

The calculation of the anharmonic IR and Raman intensities of the vibrational transitions is based on the wave-functions obtained from the VSCF or VCI methods, as recently implemented in the CRYSTAL program[x,xi]. We refer to those papers for a detailed description of the formalism. Here, we briefly recall that a VCI vibrational state *S* ($\Psi_S(Q)$) for a M dimensional system is a linear combination of the N_{conf} vibrational configurations $\Phi_N(Q)$:

$$\Psi_S(Q) = \sum_{N=1}^{Nconf} A_{N,S}\Phi_N(Q) \tag{3}$$

The $\Phi_N(Q)$ are in turn Hartree products of M one-mode functions (modals) characterized by a vibrational configuration vector *N* of the quantum numbers of each modal:

$$\Phi_N(Q) = \Phi_N(Q_1, Q_2, \dots, Q_M) = \prod_{k=1}^{M} \phi_k^{n_k(N)}(Q_k) \tag{4}$$

The modals, in turn, are expressed as a linear combination of elementary basis functions:

$$\phi_k^{n_k(N)}(Q_k) = \sum_{v_k=0}^{v_{k_{max}}} C_{v_k,n_k} \psi_k^{v_k}(Q_k) \tag{5}$$

Here the sum runs over the ten first vibrational harmonic eigenfunctions ($v_{k_{max}} = 9$) of the mode k. Two different schemes are available to set the C_{v_k,n_k} coefficients in our VCI implementation. Within the so-called VCI@HO scheme (Harmonic Oscillators basis functions), the C_{v_k,n_k} coefficients are simply set to δ_{v_k,n_k} and the $\phi_k^{n_k}$ then reduce to the corresponding harmonic modal excitations. A slightly more sophisticated ansatz is the so-called VCI@VSCF scheme (VSCF basis functions), where the coefficients are taken from a previous converged VSCF calculation on a chosen reference configuration - typically the vibrational ground state.

Anharmonic IR intensities (in km.mol^{-1}) are calculated for any IR active transition between a populated initial vibrational state $|\Psi_I\rangle$ at a temperature T, and a final state $|\Psi_F\rangle$ ($E_F > E_I$) as follows:

$$I_{I\to F}^{(IR)} \propto \sum_{a(x,y,z)=1}^{3} \left\langle \Psi_I \middle| \hat{\mu}_a \middle| \Psi_F \right\rangle^2 \tag{6}$$

Where the dipole moment $\hat{\mu}_a$ is expanded as a power series of normal coordinates:

$$\left\langle \Psi_I \middle| \hat{\mu}_a \middle| \Psi_F \right\rangle = \sum_{k=1}^{M} \left[\frac{\partial \mu_a}{\partial Q_k} \left\langle \Psi_I \middle| \hat{Q}_k \middle| \Psi_F \right\rangle + \frac{1}{2} \frac{\partial^2 \mu_a}{\partial Q_k^2} \left\langle \Psi_I \middle| \hat{Q}_k^2 \middle| \Psi_F \right\rangle + \sum_{l \neq k=1}^{M} \frac{\partial^2 \mu_a}{\partial Q_k \partial Q_l} \left\langle \Psi_I \middle| \hat{Q}_k \hat{Q}_l \middle| \Psi_F \right\rangle \right] \quad (7)$$

where $\hat{Q}_k$ is the position operator related to the k-th normal mode, and the coefficients $\frac{\partial \mu_a}{\partial Q_k} = \frac{\partial^2 E}{\partial Q_k \partial \varepsilon_a}$ are the Born charges calculated as detailed elsewhere[xii,xiii]. In our approach, the coefficients $\frac{\partial^2 \mu_a}{\partial Q_k \partial Q_l} = \frac{\partial^3 E}{\partial Q_k \partial Q_l \partial \varepsilon_a}$ are neglected (*i.e.* we consider only the mechanical part of the anharmonicity).

From **equations (3)-(5)**, we get the following working expression for $\left\langle \Psi_I \middle| \hat{\mu}_a \middle| \Psi_F \right\rangle$ (i.e. integrals of the dipole moment operator over anharmonic wavefunctions) in terms of non-vanishing integrals of position operators (in the basis of normal mode coordinates) over harmonic eigenfunctions for the calculation of the IR intensities based on the VCI@VSCF solutions:

$$\sum_{P=1}^{Nconf} \sum_{R=1}^{Nconf} A_{I,P} A_{F,R} \left\{ \sum_{k=1}^{M} \frac{\partial \mu_a}{\partial Q_k} \left[\left(\sum_{v_{k=0}}^{v_{kmax}-1} C_{v_k,n_k(P)} C_{v_k+1,n_k(R)} \left\langle \psi_k^{v_k} \middle| \hat{Q}_k \middle| \psi_k^{v_k+1} \right\rangle + \sum_{v_{k=1}}^{v_{kmax}} C_{v_k,n_k(P)} C_{v_k-1,n_k(R)} \left\langle \psi_k^{v_k} \middle| \hat{Q}_k \middle| \psi_k^{v_k-1} \right\rangle \right) \right] \prod_{l \neq k=1}^{M} \delta_{n_l(P) n_l(R)} \right\} \quad (8)$$

Let us stress that here the algorithm runs only over the populated states Ψ_I at a certain temperature T with respect to the Maxwell-Boltzmann distribution. It is thus possible to calculate the

intensities of hot bands. In the present paper, all the intensities were computed at room temperature, which do not differ from those at 0 Kelvin because of the specific wavenumbers of the lowest transitions of the molecular systems considered.

We note that IR intensities can be easily obtained from VSCF wavefunctions by considering $A_{I,P} = \delta_{I,P}$ and $A_{F,R} = \delta_{F,R}$ in the equations above, or from VCI@HO wavefunctions by considering $C_{v_k,n_k(P)} = \delta_{v_k,n_k(P)}$, $C_{v_k+1,n_k(R)} = \delta_{v_k+1,n_k(R)}$ and $C_{v_k-1,n_k(R)} = \delta_{v_k-1,n_k(R)}$.

Anharmonic Raman activities (in $Å^4amu^{-1}$) are calculated according to the Plazeck's formula[xiv]:

$$I_{I\to F}^{(Raman)} = I_{Parallel,I\to F}^{(Raman)} + I_{Perpendicular,I\to F}^{(Raman)} \tag{9}$$

$$I_{Parallel,I\to F}^{(Raman)} \propto \left(\tfrac{3}{45}B^2\right) \text{ and } I_{Perpendicular,I\to F}^{(Raman)} \propto \left(A^2 + \tfrac{4}{45}B^2\right) \tag{10}$$

Where A and B depend on the polarizability tensor α as follows:

$$A^2 = \tfrac{1}{9}\left(\langle\Psi_I|\hat{\alpha}_{xx}|\Psi_F\rangle + \langle\Psi_I|\hat{\alpha}_{yy}|\Psi_F\rangle + \langle\Psi_I|\hat{\alpha}_{zz}|\Psi_F\rangle\right) \tag{11}$$

$$B^2 = \tfrac{1}{2}\left[\left(\langle\Psi_I|\hat{\alpha}_{xx}|\Psi_F\rangle - \langle\Psi_I|\hat{\alpha}_{yy}|\Psi_F\rangle\right) + \left(\langle\Psi_I|\hat{\alpha}_{yy}|\Psi_F\rangle - \langle\Psi_I|\hat{\alpha}_{zz}|\Psi_F\rangle\right) + \left(\langle\Psi_I|\hat{\alpha}_{zz}|\Psi_F\rangle - \langle\Psi_I|\hat{\alpha}_{xx}|\Psi_F\rangle\right) + 6\left(\langle\Psi_I|\hat{\alpha}_{xy}|\Psi_F\rangle^2 + \langle\Psi_I|\hat{\alpha}_{xz}|\Psi_F\rangle^2 + \langle\Psi_I|\hat{\alpha}_{yz}|\Psi_F\rangle\right)\right] \tag{12}$$

Each term in the equations above reduces to the following expression when only the mechanical anharmonicity is taken into account, with $\frac{\partial \alpha_{ab}}{\partial q_k}$ calculated as detailed elsewhere[xv,xvi] :

$$\left\langle \Psi_I \left| \hat{\alpha}_{ab} \right| \Psi_F \right\rangle = \sum_{k=1}^{m} \left[\frac{\partial \alpha_{ab}}{\partial q_k} \left\langle \Psi_I \left| \hat{q}_k \right| \Psi_F \right\rangle \right] \quad \text{with} \quad \frac{\partial \alpha_{ab}}{\partial q_k} = \frac{\partial^3 E}{\partial q_k \partial \varepsilon_a \partial \varepsilon_b} \tag{13}$$

Hence, the anharmonic Raman activities can be computed separately for each component of the polarizability tensor:

$$I_{ab,I\to F}^{(Raman)} \propto \left\langle \Psi_I \left| \hat{\alpha}_{ab} \right| \Psi_F \right\rangle^2 \tag{14}$$

This yields to explicit expressions for the Raman activities (not reported for brevity) similar to **equation (8)** for IR intensities where VSCF, VCI@HO or VCI@VSCF wavefunctions can be considered.

As a final comment, it is worth stressing that intensities/activities from a purely VSCF wave-function are zero by essence for combination bands given that a VSCF wavefunction describes the states of an oscillator as a linear combination of its own multi-excitations, which can be seen as an intrinsic anharmonicity. Only the inclusion of multiple configurations, as achieved

within the VCI approach, can provide the missing bands and a better estimation of the amplitudes of the overtones as well by taking into account the so-called extrinsic anharmonicity.

COMPUTATIONAL DETAILS

All calculations are performed with a developmental version of the CRYSTAL17 program, where the methodologies presented in Section II have been implemented[xvii]. Four systems are considered: two molecules (water, H_2O, and formaldehyde, H_2CO) and two solids (cubic sodium and potassium boron-hydrides, $NaBH_4$ and KBH_4, respectively including the deuterated species $NaBD_4$ and KBD_4).

Concerning the water and formaldehyde molecules, the aug-cc-pVTZ[xviii] basis set was used with the B3LYP[xix,xx,xxi,xxii] hybrid functional of the density functional theory. For $KBH(D)_4$ and $NaBH(D)_4$, two basis sets were used: the one hereafter indicated as B1 in which the 6-31G(d,p)[xxiii] basis set for H and B and the pob_TZVP_2012[xxiv] basis set for K and Na were considered and the basis set indicated as B2, the pob_TZVP_2012[24] basis set was used for H, B, K and Na. For the crystalline systems the B3LYP and the PBEsol0 hybrid functionals were used[xxv]. In particular, the B3LYP functional was adopted because of its well-documentedability to reproduce experimental fundamental transitions with an average deviation of about 10 cm^{-1} for semi rigid molecules[xxvi].

The DFT exchange-correlation contribution is evaluated by numerical integration over the unit cell volume. Radial and angular points of the integration grid are generated through Gauss-Legendre radial quadrature and Lebedev two-dimensional angular point distributions. A pruned grid corresponding to 75 radial and 974 angular points, was employed. Evaluation of the Coulomb and exchange interactions is controlled by five parameters, whose values are set to T1=T2=T3=T4=½T5=TI. In this work we used TI=10 and a shrinking factor (for sampling in

reciprocal space) of 4. The latter value was chosen after having performed a series of calculations using different shrinking factors ranging from 2 to 8, and after having observed that results obtained with 4 do not deviate by more than 0.3 cm^{-1} for the harmonic wavenumbers and 0.5% for the harmonic intensities with respect to 8.

Concerning the harmonic computations of IR intensities and Raman activities, the Coupled Perturbed Kohn-Sham (CPKS) scheme is used[12,13,15,16].

The convergence of the SCF process is checked on the energy, with a threshold of 10^{-10} hartree between two consecutive iterations. The convergence of the CPKS iterative process is controlled by a threshold on the polarizability of 10^{-4} $bohr^3$.

Third- and fourth-order energy derivatives with respect to atomic displacements around the equilibrium geometry were computed following the numerical scheme 4 described in our previous work[10]. Here we just recall that this scheme allows for the evaluation of the cubic and quartic terms of one-, two- and three-mode interactions. In addition to the equilibrium structure for which the Hessian is computed, the number of configurations where the energy and gradients are computed is four for each normal mode plus other four for each pair of modes.

Moreover, the step size between each point is 1.0 time the classical amplitude of each mode[10]. Concerning this point, a preliminary investigation of the most effective step size to be used was performed from anharmonic computations of wavenumbers and intensities on KBH_4 species for testing different step sizes both in terms of classical amplitude and variation of the atomic positions in the ranges [0.4-1.6] and [0.1-0.5] Å, respectively. This revealed that even though the values of the anharmonic positions differ by less than 2 cm^{-1} in the ranges, the anharmonic IR intensities (and then the weighted coefficient of the anharmonic wave functions, see section II) remain more stable in the ranges [0.8-1.2] and [0.15-0.25] for the two options of step size. Note however that the $MBH(D)_4$ species do not have low frequency modes (below 400 cm^{-1}).

The anharmonic vibrational levels[11] were calculated within the VCI@VSCF formalism and the VCI expansion was truncated according to the maximum number of modes simultaneously excited (N_{modes}=4) and the maximum excitation level (N_{quanta}=6) with respect to the fundamental VSCF state. This yields VCI matrices containing up to the fourth excitations of the doubly-excited VSCF states, that corresponds to the so-called VCI@VSCF[4] in the notation proposed in ref.6 and therein. This allows for a converged calculation for the fundamental transitions, first-overtones and combination bands involving two quanta[11]. It should be remembered (see ref.11) that a VCI treatment yields the same converged values whatever the reference used for their computations (HO or VSCF), however, the VCI@VSCF approach converges faster than the VCI@HO one, thus requiring smaller VCI matrices to be built and diagonalized.

The shapes of the vibrational spectra illustrated in the present paper were built from the values of the anharmonic positions and intensities fitted by Lorentzian functions of 10 cm^{-1} width. This value was set in order to reproduce qualitatively the shape of the experimental spectra of KBH_4 and $NaBH_4$ illustrated in ref. xxvii.

RESULTS AND DISCUSSION

In this section, we address the quality of the theoretical values for anharmonic IR intensities and Raman activities obtained with the present implementation. Theoretical and experimental data on the two molecular systems (water H_2O and formaldehyde H_2CO) are reported in **Tables 1 and 2**, respectively. Seidler et al. in ref. 6 employed a VCI@VSCF treatment based on a B3LYP/aug-cc-PVTZ quartic force field for which VCI matrix sizes similar to ours were considered (see section “Computational Details”). The reliability of the anharmonic wavenumbers was commented in a previous work[11]. We note that, at variance with the periodic case, the rotational contribution to anharmonicity[xxviii] can be non-negligible for small molecules. Hence,

rotationally-corrected values are added to the table in parenthesis for better estimation of the possible error sources. These values were computed with the VCI-P code[xxix]. Passing to IR intensities and Raman activities, the present implementation includes only the first derivatives of the related operator with respect to the atomic displacements. This leads to some discrepancies with respect to previous theoretical results in the literature, namely for the IR intensities ($I^{(IR)}$ in table I and II) and particularly for the $2\nu_2$, $\nu_2+\nu_1$, $\nu_2+\nu_3$ and $2\nu_2$, $2\nu_3$, $\nu_2+\nu_4$ for H_2O and H_2CO respectively. Anyway, a purely variational treatment of the anharmonicity performed with the VCI-P code[29] and based on the same force field adopted here, yields theoretical results identical to those of our study or in line with the other reported values, depending on whether the use of second derivatives of the dipole moment were disabled or not (in parenthesis in the tables).

Table 1: VCI@VSCF anharmonic frequencies and anharmonic IR intensities and Raman activities (in $km.mol^{-1}$ and $Å^4.amu^{-1}$, respectively) using a B3LYP/aug-cc-pVTZ quartic force field for H_2O and comparison to experimental data.

	This study : VCI@VSCF[4]				VCI@VSCF[3][a]				Exp.[a]		
	ν^b	$I^{(IR)c}$	$I^{(RA)}$		ν	$I^{(IR)}$	$I^{(RA)}$		ν	$I^{(IR)}$	$I^{(RA)}$
ν_2	1548 (1562)	76.3 (76.3)	1.10		1552	76.6	1.26		1595	53.6-71.9	0.9±0.2
ν_1	3665 (3666)	3.72 (3.75)	102		3669	3.59	109		3657	2.24-2.98	111±12
ν_3	3738 (3756)	61.3 (61.1)	27.0		3751	58.3	28.8		3756	41.7-44.6	19±2
$2\nu_2$	3048 (3075)	0.01 (0.46)	1.10		3061	0.34	0.07		3152	0.461	
$2\nu_1$	7301 (7303)	0.07 (0.16)	0.50		7316	0.31	0.12		7202	0.32	
$2\nu_3$	7430 (7451)	0.06 (0.13)	0.30		7479	0.00	0.12		7468	0.032	
$\nu_2+\nu_1$	5169 (5184)	0.01 (0.23)	0.10		5176	0.08	0.38		5235	0.223	
$\nu_2+\nu_3$	5217 (5266)	0.61 (3.11)	0.20		5232	3.93	0.00		5331	4.5	
$\nu_1+\nu_3$	7354 (7362)	1.15 (1.56)	0.30		7389	2.65	0.01		7250	4.85	

[a]: see ref. 6
[b]: anharmonic wavenumbers without and with (in parenthesis) the rotational contribution to anharmonicity.
[c]: anharmonic IR intensities without and with (in parenthesis) the use of the second derivatives of the dipole moment.

Table 2: VCI@VSCF anharmonic frequencies and anharmonic IR intensities, and Raman activities (in km.mol^{-1} and Å^4.amu^{-1}, respectively) using a B3LYP/aug-cc-pVTZ quartic force field for H_2CO and comparison to experimental data.

	This study : VCI@VSCF[4]				VCI@VSCF[4][a]				Exp.[a]	
	ν^b	$I^{(IR)c}$	$I^{(RA)}$		ν	$I^{(IR)}$	$I^{(RA)}$		ν	$I^{(IR)}$
ν_4	1165 (1179)	5.74 (5.86)	0.30		1162	5.55	0.49		1167	5.5-6.5
ν_6	1233 (1237)	12.7 (13.0)	0.80		1234	12.4	1.54		1249	9.4-9.9
ν_3	1487 (1489)	18.6 (18.7)	11.6		1491	10.4	10.9		1500	11.2
ν_2	1787 (1788)	108. (108.)	7.00		1786	120.	11.0		1746	74.0
ν_1	2743 (2746)	68.7 (78.7)	184		2743	75.6	263		2782	48-75
ν_5	2814 (2823)	59.5 (80.5)	56.5		2795	97.0	101		2843	59-88
$2\nu_4$	2327 (2354)	1.45 (0.25)	5.20		2320	0.18	0.89		2327	0.14
$2\nu_6$	2463 (2472)	1.14 (0.56)	4.40		2464	0.58	1.31		2493	0.27
$2\nu_3$	2970 (2974)	0.07 (1.62)	0.00		3020	2.05	4.61		3000	2.2-2.5
$2\nu_2$	3561 (3563)	0.75 (4.23)	0.00		3555	4.31	0.97		3472	3.80
$\nu_3+\nu_4$	2669 (2686)	0.00 (0.02)	0.00		2652	0.02	0.04		2656	0.04
$\nu_3+\nu_6$	2674 (2682)	51.3 (47.6)	53.4		2686	36.4	46.5		2719	8-14
$\nu_2+\nu_4$	2960 (2976)	0.00 (0.47)	0.00		2941	0.48	0.15		2905	2.3
$\nu_2+\nu_6$	3041 (3046)	4.77 (5.67)	4.30		3019	3.48	5.41		3000	0.5-10
$\nu_2+\nu_3$	3284 (3287)	0.00 (0.03)	0.57		3270	0.17	1.23		3238	-

[a]: see ref. 6
[b]: anharmonic wavenumbers without and with (in parenthesis) the rotational contribution to the anharmonicity.
[c]: anharmonic IR intensities without and with (in parenthesis) the second derivatives of the dipole moment.

Now we discuss results on periodic systems. Boron hydrides $BH(D)_4^-$ in a crystalline environment of alkali metals (M=Na,K) (see **Figure 1**) constitute an excellent example for the validation of the present implementation. Indeed, for these species, one of the first overtones and a combination band of $BH(D)_4^-$ are known to be highly active because of strong interactions with a fundamental transition of the molecule[8], as sketched in **Figure 2**. The strong mode-mode couplings between the mode ν_3(F2) (asymmetric stretching mode), the combination mode ν_2(E)+ν_4(F2) (symmetric + asymmetric bending modes) and the overtone mode $2\nu_4$(F2) lead to significant amplitudes for the corresponding transitions. The interaction between the $2\nu_4$ and ν_3 vibrational states is so strong and their energies at first-order (labeled ν^0_i in **Figure 2** and corresponding to the diagonal terms of the VCI matrix, *i.e.* without the consideration of mode-mode couplings) are so close that a small perturbation (such as the nature of the alkali metal in the crystalline framework) can easily change their relative first-order ranking in energy. As a consequence, the amplitude ratio between the two corresponding transitions and their labelling are also strongly dependent on the nature of the alkali metal.

Figure 1: Cell geometry of the face-centered cubic $MBH(D)_4$ species (M=Na,K)

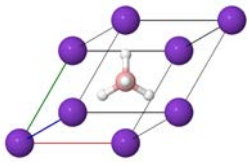

Figure 2: Qualitative energetic diagrams and corresponding vibrational spectra of the three vibrational states interacting in the stretching region for $MBH(D)_4$ species. (ν^0 are the solutions of the first-order perturbation theory, i.e. diagonal terms of the VCI matrix).

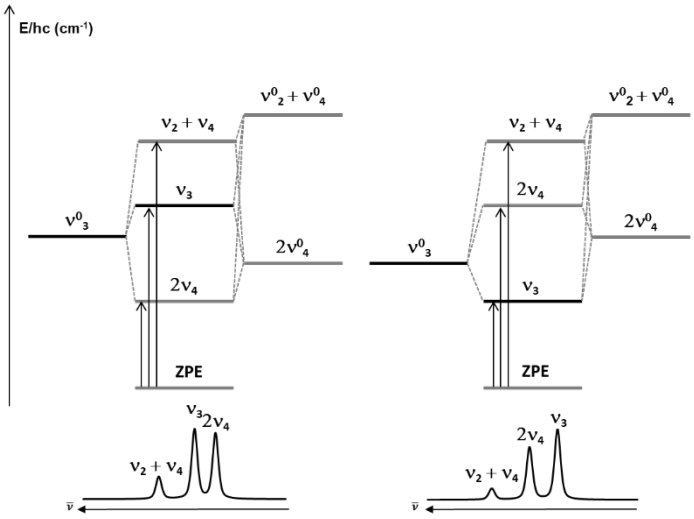

The computed anharmonic vibrational signature of such species is strongly dependent on the first order results - especially when small energy differences are involved (about 10 cm^{-1} for the present example) - and hence, on the choice of the electronic structure calculation. This is illustrated in **Figure 3** in which the anharmonic IR signature in the stretching region of KBH_4 is obtained from the B3LYP and the PBEsol0 functionals in combination with the B1 and B2 basis sets. As regards the comparison with the experimental counterpart[27], it can be observed that the PBEsol0 functional results in a better agreement than B3LYP in terms of relative peak intensities, with both basis sets. On this point, we mention that the inclusion of the second derivatives of the dipole moment with the use of the VCI-P code (see the paragraph concerning the molecular cases) does not significantly modify the values of the IR intensities in this case.

The PBEsol0 functional will be used hereafter. The effect of the basis set is less straightforward because B1 provides the best peak positions ($\Delta\nu_{PBEsol0/B1-EXP}(2\nu_4)$=-15; $\Delta\nu_{PBEsol0/B1-EXP}(\nu_3)$=+10; $\Delta\nu_{PBEsol0/B1-EXP}(\nu_2+\nu_4)$=+3 versus $\Delta\nu_{PBEsol0/B2-EXP}(2\nu_4)$=+49; $\Delta\nu_{PBEsol0/B2-EXP}(\nu_3)$=+42; $\Delta\nu_{PBEsol0/B2-EXP}(\nu_2+\nu_4)$= +58 -in cm^{-1}-) while B2 provides the best peak shapes. This being said, a further optimization of basis sets or scale factors would be possible but is beyond the scope of this paper.

Figure 3: Anharmonic IR spectrum of KBH_4 in the stretching region obtained from four DFT models with the corresponding experimental information. The experimental counterpart has been redrawn from experimental positions and amplitudes reported in ref. 27, by following the same numerical treatment detailed in section "Computational Details" used for our computed data.

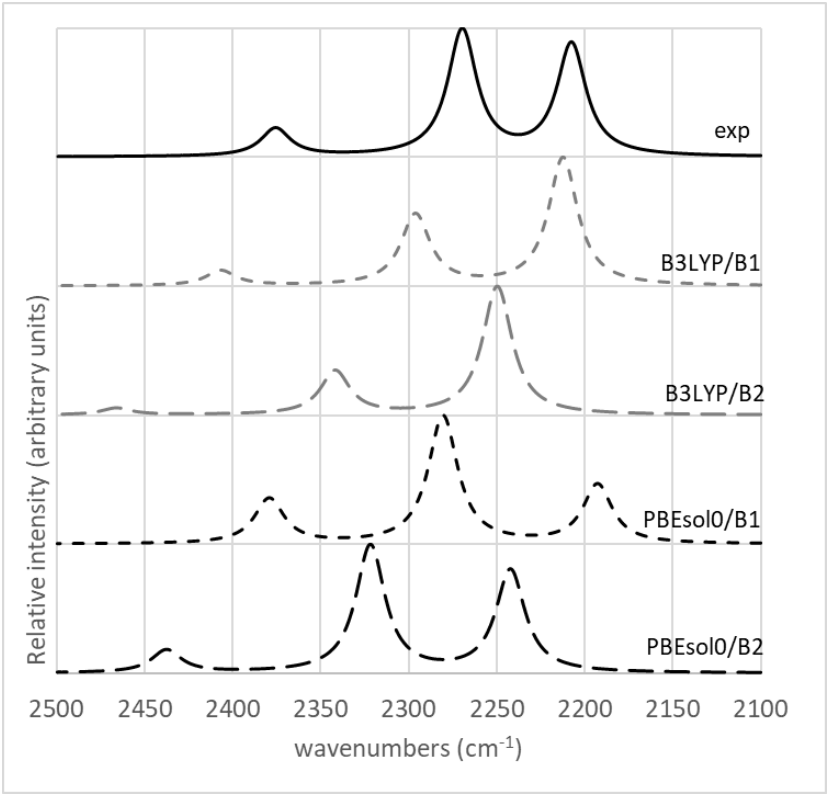

Figures 4 and 5 display the simulated IR and Raman spectra of the stretching region of MBH_4 and MBD_4 species, respectively (M=Na or K). Experimental and theoretical spectra from

PBEsol0/B1 and PBEsol0/B2 models are reported in insets labelled EXP, B1 and B2, respectively. The bottom curves of each panel report the harmonic spectra. Anharmonicity is crucial in order to get the correct description of the spectra in this case. Note that the harmonic IR spectrum only exhibits one feature, while in the experiment we have three. Furthermore, the harmonic Raman spectrum only exhibits two features, while in the experiment we have six. So, two out of three spectral features are due to anharmonicity in the IR spectrum and four out of six in the Raman spectrum. The transitions marked as filled squares ($2\nu_4$(F2)), pentagons (ν_3(F2)), or hexagons ($\nu_2+\nu_4$(F2)) are both IR and Raman active while those marked as filled four-pointed stars ($2\nu_4$(A1)), five-pointed stars (ν_1(A1)) or six-pointed stars ($2\nu_2$(A1)) are Raman active only. Moreover, black symbols refer to $NaBH(D)_4$ while grey symbols refer to $KBH(D)_4$.

The first consideration that can be made is the following: an account of the mechanical part of the anharmonicity (based on a representation of the PES including up to fourth-order terms) allows for the correct qualitative identification of all IR and Raman active transitions. However, a closer look at the computed spectra reveals that the choice of a good quantum-chemical model for the electronic structure calculations (exchange-correlation functional and basis set) is crucial in order to get the correct quantitative description in terms of relative peak positions, relative peak intensities, and peak assignment. This is expected in this case as a difficult balance is to be found between the strong Fermi resonances producing some spectral features and the much weaker interactions responsible for the small satellite peaks around some active fundamental transition.

Figure 4: Computed IR and Raman spectra of KBH_4 and $NaBH_4$ in the stretching region, as compared with the experimental counterpart (ordinate: intensity in arbitrary units; abscissa: wave-numbers in cm^{-1}). See text for more details. Anharmonic (I_{anharm}) and harmonic (I_{harm}) spectra are provided. The PBEsol0 functional is used.

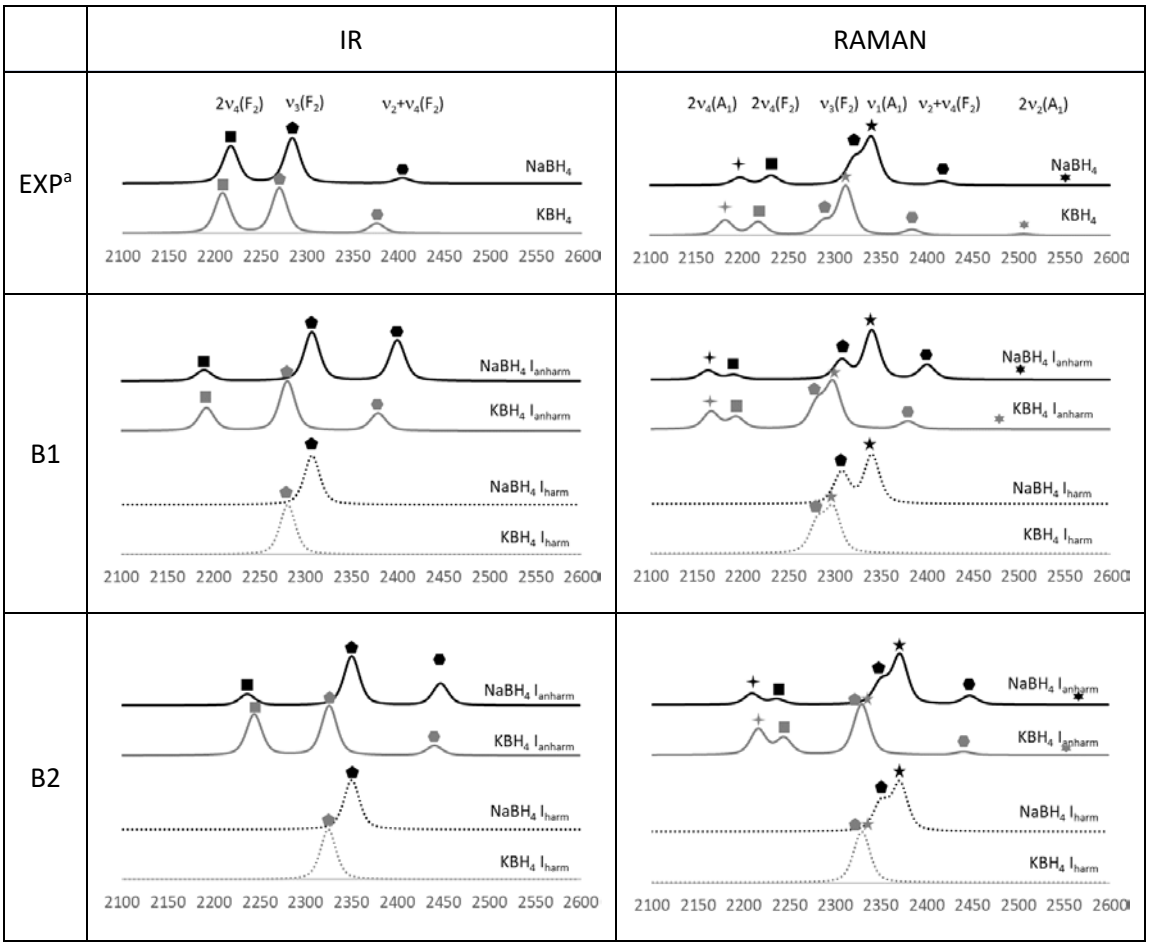

[a]: without the positions and amplitudes related to $M^{10}BH_4$, see also section III for the numerical treatment of the positions and intensities taken from ref. 27.

We start by illustrating a case where the adopted quantum-chemical model works extraordinarily well. All features (relative peak positions, intensities, and assignment) of IR and Raman spectra of both KBH_4 and KBD_4 are nicely reproduced with the PBEsol0/B2 model. The analysis of the corresponding VCI wavefunctions shows that this is mainly due to the correct description of the ω_3 character in the $2\nu_4(F2)$, $\nu_3(F2)$, $\nu_2+\nu_4(F2)$ states and of the ω_1 character in the $2\nu_4(A1)$, $\nu_1(A1)$, $2\nu_2(A1)$ states. This enables the correct assignment of the bands in the IR and Raman spectra of both KBH_4 and KBD_4 in their stretching region. As a final comment on this case, we note that the computed spectra are shifted by about 30-50 cm^{-1} with respect to the experimental ones but this is of little concern when it comes to assigning the spectral features.

Figure 5: Computed IR and Raman spectra of deuterated species KBD_4 and $NaBD_4$ in the stretching region, as compared with the experimental counterpart (ordinate: intensity in arbitrary units; abscissa: wave-numbers in cm^{-1}). See text for more details. Anharmonic (I_{anharm}) and harmonic (I_{harm}) spectra are provided. The PBEsol0 functional is used.

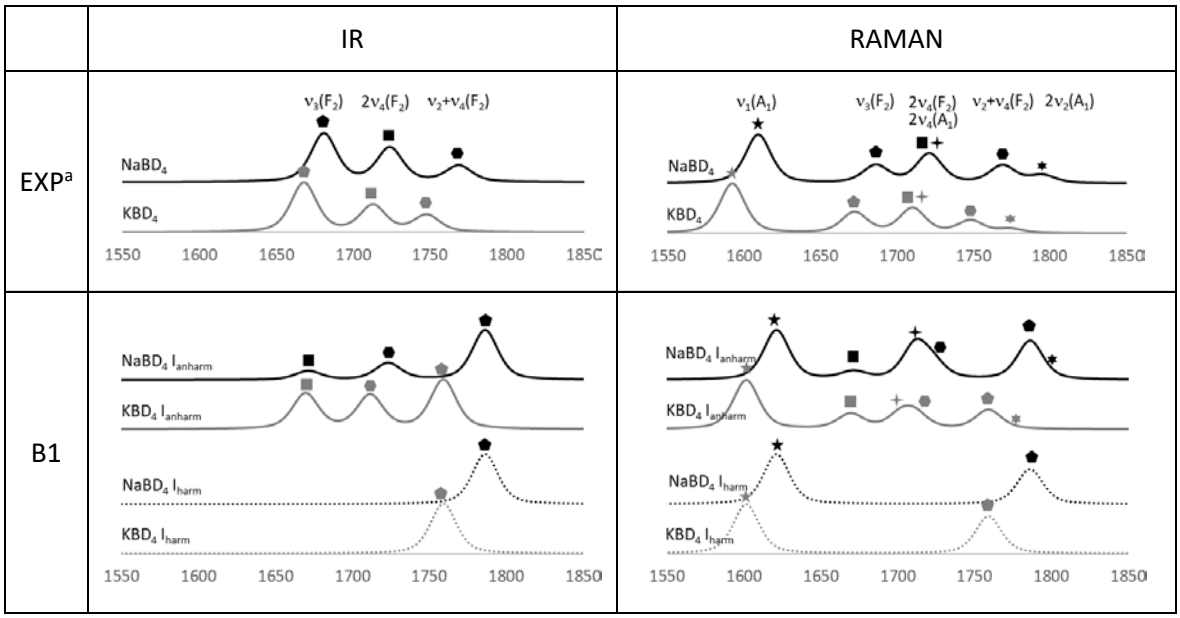

B2	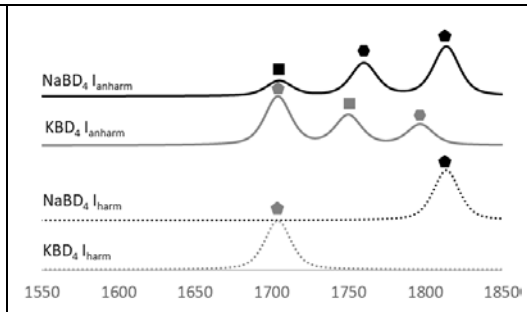	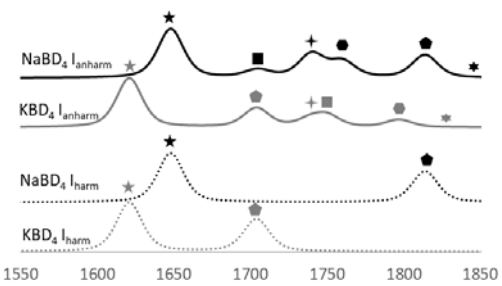

[a]: without the positions and amplitudes related to $M^{10}BD_4$, see also section III for the numerical treatment of the positions and intensities taken from ref. 27.

The description obtained for the $NaBH_4$ and $NaBD_4$ species is slightly less satisfactory. This is particularly true for the deuterated species. On the one hand, also for these systems, the right number of active spectral features is obtained (three for IR and six for Raman). On the other hand, for $NaBH_4$, the computed spectra are slightly off in terms of relative peak positions and relative intensities but not to an extent to prevent a correct assignment. On the contrary, for $NaBD_4$, the description is more problematic and leads to the wrong assignment of many spectral features.

Despite the limitations due to the need for a carefully tuned quantum-chemical model for the electronic structure calculations (for the description of the PES), we think we have shown how the description of strongly anharmonic vibrational spectra can be significantly improved over the commonly-used harmonic approximation with the present methodology. Note that even the very weak transitions (marked with six-pointed stars in the simulated spectra of **Figures 4 and 5**) could be correctly identified, thus providing enough additional information to exclude that they could be due to impurities in the experimental spectra.

CONCLUSIONS AND PERSPECTIVES

We have presented the implementation in the public CYSTAL program of a computational scheme for the calculation of anharmonic IR intensities and Raman activities for periodic systems. To the best of our knowledge, this represents the first implementation of such a feature in a solid state context. The approach relies on the evaluation of integrals of the dipole moment and polarizability operators over anharmonic wavefunctions obtained from VSCF, VCI@HO or VCI@VSCF calculations for the anharmonic vibrational states. Thus, it becomes possible not only to correct for anharmonic effects the intensities of those fundamental transitions already present at the harmonic level, but also to compute the intensity of overtones and combination bands, whose non-vanishing values are due to mode-mode couplings.

For validation purposes, we have reported results on two simple molecular cases, H_2O and H_2CO, and compared them to previous data from the literature. The method based on a variational VCI wavefunction can treat both the weakest couplings, which yield the satellite peak(s) in the vicinity of a fundamental transition, and the strongest couplings (typically called Fermi resonances) yielding overtones and combination bands that can be as intense as their corresponding fundamental transitions.

We have applied our methodology to the study of the anharmonicity in the B-H stretching region of boron hydrides in a crystalline environment of alkali metals (M=Na, K): MBH_4 and the deuterated counterpart MBD_4, for which accurate experimental spectra are available for comparison. We think that this system constitutes an excellent test for the present methodology. Two out of the three IR spectral features are due to anharmonicity, and four out of the six Raman spectral features are due to anharmonicity. All these anharmonic spectral features could be successfully identified and assigned.

It is worth stressing that, for systems exhibiting low-frequency vibrational motions (with wavenumbers below, say, a few hundreds of cm^{-1}, in particular torsional modes or hindered rotations), a more flexible representation of the PES with respect to the current one would be mandatory for reliable anharmonic computations of their vibrational transitions. Work has already been done in this direction in a molecular context (for the evaluation of five-to-eight order force-constants in the polynomial representation of the PES in Taylor series).[xxx,xxxi] Work is in progress for an automated procedure able to select a restricted set of modes and mode-mode couplings in order to build a reliable reduced PES. These developments will also need to be complemented by those devoted to the treatment of the electrical anharmonicity from the computation of third- and fourth-order derivatives of the energy with respect to the normal modes and electrical field. These aspects constitute some step-by-step developments required to improve the quality of the results in this research area in order to propose a general-purpose computational tool for vibrational anharmonicity of solids.

AUTHOR INFORMATION

Corresponding Author

*Philippe Carbonniere, philippe.carbonniere@univ-pau.fr.

ACKNOWLEDGMENTS

P.C. and M.R. gratefully acknowledge GENCI (Grand Equipement National de Calcul Intensif) for computing facilities through project number A0030810320 at TGCC/Irène (Très Grand Centre de Calcul) CEA, France.

REFERENCES

[i] Torré, J. P. ; Coupan, R.; Chabod, M.; Père, E.; Labat, S.; Khoukh, A.; Brown, R.; Sotiropoulos, J. M.; Gornitzka, H. CO_2-Hydroquinone Clathrate : Synthesis, Purification, Characterization and Crystal Structure. *Cryst. Growth. Des.* **2016**, 16, 5330-5338.

[ii] Greve, C.; Preketes, N. K.; Fidder, H.; Costard, R.; Koeppe, B.; Heisler, I. A.; Mukamel, S.; Temprs, F.; Nibbering, E. T. J.; Elsaesser, T. N-H Stretching Excitations in Adenosine-Thymidine Base Pairs in Solution: Base Pair Geometries, Infrared Line Shapes and Ultrafast Vibrational Dynamics. *J. Phys. Chem. A.* **2013**, 117, 594-606.

[iii] Ryskin, Y. I. The Vibrations of Protons in Minerals: Hydroxyl, Water and Ammonium, in The Infrared Spectra of Minerals, edited by V. C. Farmer (Mineralogical Society of America), **1974**, 137-181.

[iv] Carteret, C.; De La Pierre, M.; Dossot, M.; Pascale, F.; Erba, A.; Dovesi, R. The Vibrational Spectrum of CaCO3 Aragonite : a Combined Experimental and Quantum-Mechanical Investigation. *J. Chem. Phys.* **2012**, 138, 014201.

[v] White, W. B. The Carbonate Minerals, in The Infrared Spectra of Minerals, edited by V. C. Farmer (Mineralogical Society of America), **1974**, 227-284.

[vi] Seidler, P.; Kongsted, J.; Christiansen, O. Calculation of Vibrational Infrared Intensities and Raman Activities Using Explicit Anharmonic Wave Functions. *J. Phys. Chem. A.* **2007**, 111, 11205-11213.

[vii] Burcl, R.; Carter, S.; Handy, N. C. Infrared Intensities from the Multimode Code. *Chem. Phys. Lett*. **2003**, 380, 237-244.

[viii] Harvey, K. B.; McQuaker, N. R. Infrared and Raman Spectra of Potassium and Sodium Borohydride. *Can. J. Chem.* **1971**, 49, 3272-3281.

[ix] Carbonniere, P.; Hagemann, H. Fermi Resonances of Borohydrides in a Crystalline Environment of Alkali Metals. *J. Phys. Chem. A.* **2006**, 110, 9927-9933.

[x] Erba, A.; Maul, J.; Ferrabone, M.; Carbonnière, P.; Rerat, M.; Dovesi, R. Anharmonic Vibrational States of Solids from DFT Calculations. Part I: Description of the Potential Energy Surface. *J. Chem. Theory Comput*. **2019**, 15, 3755-3765.

[xi] Erba, A.; Maul, J.; Ferrabone, M.; Dovesi, R.; Rerat, M.; Carbonnière, P. Anharmonic Vibrational States of Solids from DFT Calculations. Part II: Implementation of the VSCF and VCI methods. *J. Chem. Theory Comput*. **2019**, 15, 3766-3777.

[xii] Maschio, L.; Kirtman, B.; Orlando, R.; Rerat, M. Ab Initio Analytical Infrared Intensities for Periodic Systems Through a Coupled Perturbed Hartree-Fock/Kohn-Sham Method. *Chem. Phys.* **2012**, 137, 204113.

[xiii] Maschio, L.; Kirtman, B.; Rerat, M.; Orlando, R.; Dovesi, R. Comment on "Ab Initio Analytical Infrared Intensities for Periodic Systems Through a Coupled Perturbed Hartree-Fock/Kohn-Sham Method" [J. Chem. Phys.137, 204113 (2012)]. *J. Chem. Phys.* **2013**, 139, 167101.

[xiv] Schrader, B.; Moore, D. S. Laser-Based Molecular Spectroscopy for Chemical Analysis-Raman Scattering Processes. *Pure & Appl. Chem.* **1997**, 69, 1451-1468.

[xv] Maschio, L.; Kirtman, B.; Rerat, M.; Orlando, R.; Dovesi, R. Ab Initio Analytical Raman Intensities for Periodic Systems Through a Coupled Perturbed Hartree-Fock/Kohn-Sham Method in an Atomic Orbital Basis. I. Theory. *J. Chem. Phys.* **2013**, 139, 164101.

[xvi] Maschio, L.; Kirtman, B.; Rerat, M.; Orlando, R.; Dovesi, R. Ab Initio Analytical Raman Intensities for Periodic Systems Through a Coupled Perturbed Hartree-Fock/Kohn-Sham Method in an Atomic Orbital Basis. II. Validation and Comparison with Experiments. *J. Chem. Phys.* **2013**, 139, 164102.

[xvii] Dovesi, R.; Erba, A.; Orlando, R.; Zicovich-Wilson, C. M.; Civalleri, B.; Maschio, L.; Rerat, M.; Casassa, S.; Baima, J.; Salustro, S.; Kirtman, B. *WIREs Comput. Mol. Sci*. **2018**, 8, e1360.

[xviii] Kendall, R. A.; Dunning Jr, T. H.; Harrison, R. J. Electron Affinities of the First-row Atoms Revisited. Systematic Basis Sets and Wave Functions. *J. Chem. Phys.* **1992**, 96, 6796-6806.

[xix] Becke, A. D. Density-Functional Thermochemistry III. the Role of Exact Exchange. *J.Chem.Phys.* **1993**, 98, 5648-5652

[xx] Lee, C.; Yang, W.; Parr, R. G. Development of the Colle-Salvetti Correlation-Energy Formula Into a Functional of the Electron Density. *Phys. Rev. B* **1988**, 37, 785-789

[xxi] Vosko, S. H.; Wilk, J.; Nusair, M. Accurate Spin-Dependent Electron Liquid Correlation Energies for Local Spin Density Calculations: a Critical Analysis. *Can. J. Phys.* **1980**, 58, 1200-1211

[xxii] Stephens, P. J.; Devlin, F. J.; Chabalowski, C. F.; Frisch, M. J. Ab Initio Calculation of Vibrational Absorption and Circular Dichroism Spectra Using Density Functional Force Fields. *J. Phys. Chem.* **1994**, 98, 11623-11627

[xxiii] Hariharan, P. C.; Pople, J. A. The Influence of Polarization Functions on Molecular Orbital Hydrogenation Energies. *Theoret. Chim. Acta* **1973**, 28, 213-222.
[xxiv] Peintinger, M. F.; Vilela Oliveira, D.; Bredow T. Consistent Gaussian Basis Sets of Triple-Zeta Valence with Polarization Quality for Solid-State Calculations. *J. Comput. Chem*. **2012**, 34, 451-459.
[xxv] Perdew, J. P.; Ruzsinsky, A.; Csonka, G. I.; Vydrov, O. A.; Scuseria, G. E.; Constantin, L. A.; Zhou, X.; Burke, K. Restoring the Density-Gradient Expansion for Exchange in solids and Surfaces. *Phys. Rev. Lett.* **2008**, 100, 136406.
[xxvi] Carbonniere, P.; Lucca, T.; Pouchan, C.; Rega, N.; Barone, V. Vibrational Computations Beyond the Harmonic Approximation: Performances of the B3LYP Density Functional for Semirigid Molecules. *J. Comput. Chem.* **2005**, 26, 384-388.
xxvii Renaudin, G.; Gomes, S.; Hagemann, H.; Keller, L.; Yvon, K. Structural and Spectroscopic Studies on the Alkali Borohydrides MBH_4 (M=Na, K, Rb, Cs). *J. Alloys compd.* **2004**, 375, 98-106.
[xxviii] Carbonniere, P.; Barone, V. Coriolis Couplings in Variational Computations of Vibrational Spectra Beyond the Harmonic Approximation: Implementation and Validation. *Chem. Phys. Lett*. **2004**, 392, 365-371.
[xxix] Carbonniere, P.; Dargelos, A.; Pouchan, C. The VCI-P Code: An Iterative Variation-Perturbation Scheme for Efficient Computations of Anharmonic Vibrational Levels and IR Intensities of Polyatomic Molecules. *Theo. Chem. Acc.* **2010**, 125, 543-554.
[xxx] Richter, F.; Thaunay, F.; Lauvergnat, D.; Carbonniere, P. Anharmonic Vibrational Treatment Exclusively in Curvilinear Valence Coordinates: the Case of Formamide. *J. Phys. Chem. A* **2015**, 119, 11719-11728.
[xxxi] Richter, F.; Carbonniere, P. Vibrational Treatment of the Formic Acid Double Minimum Case in Valence Coordinates. *J. Chem. Phys.* **2018**, 148, 064303.